Lamb wave contrast in non-contacting surface acoustic wave microscopy

M.G. Somekh, S.D. Sharples, M. Clark and C.W. See

Subsurface imaging in a non-contacting surface acoustic wave microscope is demonstrated, using mode conversion from Rayleigh to Lamb modes. The fact that, unlike in a conventional acoustic microscope, the technique does not require fluid couplants allows new contrast mechanisms to be used for the quantification of defects.

Introduction: There is no doubt that laser ultrasonics will become even more important and used more routinely in non-destructive testing in the next decade. In an earlier Letter [1] we showed how a non-contacting surface acoustic wave microscope could be produced by combining fast analogue detection electronics with a computer-generated hologram to produce an optical distribution, which acts as a source for focused surface waves. We demonstrated similar imaging performance to that of a fluid coupled acoustic microscope. The system was, of course, non-contact and non-destructive. We showed that interference fringes between forward and back propagating Rayleigh waves were a characteristic feature of images close to a reflecting defect. These features are an exact analogue of the interference fringes found in the fluid coupled acoustic microscope [2].

In this Letter we demonstrate that the non-contacting surface acoustic wave microscope is capable of producing useful surface wave contrast mechanisms, which cannot be produced using fluid-based scanning acoustic microscopes.
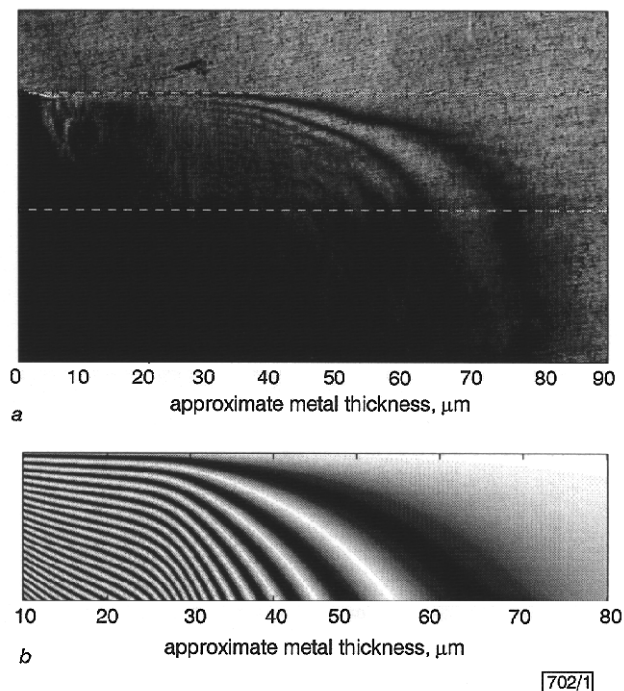

Fig. 1 *Surface wave image and calculated interference pattern*

a 82 MHz surface wave image obtained over subsurface wedge demonstrating Lamb wave interference; full width of image 5 mm; sound propagation direction from top to bottom
– – – – position of subsurface wedge
b Calculated interference pattern arising from interference of Lamb waves on aluminium sample

Examples of Lamb wave contrast: In the proposed system, surface acoustic waves are produced in an arc and come to a geometric focus, where the resulting surface displacement is detected with a specialised knife-edge detector. For the results presented in this Letter the arc focal length was 2 mm to reduce the effects of acoustic speckle [3], and the semi-angle for excitation was 30°. The sample was scanned across a tapered subsurface wedge. The surface wave image obtained at 82 MHz is shown in Fig. 1*a*. Excitation of the surface waves occurs above the wedge, where the sample is thick; this means that only Rayleigh waves are excited on the surface. We further ensured that only Rayleigh waves were excited as we used multiple arcs to excite waves in a narrow velocity range. As the Rayleigh waves hit the interface between the solid

material and the wedge they are mode converted to Lamb waves. The difference in velocity between the symmetric and the antisymmetric Lamb waves is a function of the thickness of the sample [4]. When the sample is thick, as on the right hand side of Fig. 1, the two waves will have similar velocities close to the Rayleigh wave velocity. As the thickness decreases the velocity of the symmetric wave increases and that of the antisymmetric wave decreases. The characteristic fringes in Fig. 1*a* are produced by interference between symmetric and antisymmetric Lamb modes; the period of the ripple increases as the thickness increases because both velocities approach the Rayleigh wave velocity and the beat length increases. Fig. 1*b* shows the calculated fringe pattern formed from the interference between two forward propagating symmetric and antisymmetric Lamb waves. The agreement between experiment and theory indicates that the fringe spacing is an effective means for quantitative determination of the material thickness in the wedge.
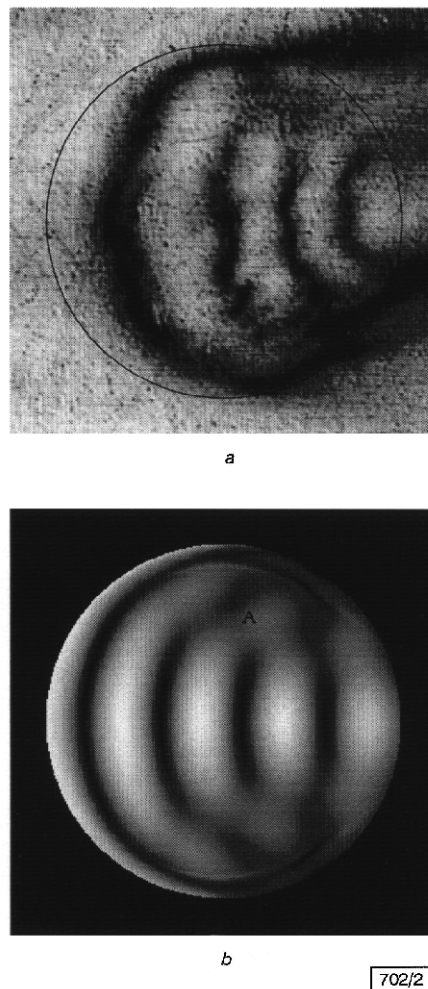

Fig. 2 *Surface wave image and simulated image of defect*

a 82 MHz surface wave image obtained over 1 mm subsurface hole indicated by circle; sound propagation direction from left to right
b Simulated image of defect of uniform thickness and 36 μm deep; fringe contrast is reduced in region A

We have also imaged samples with circular defects. These were formed by drilling to different depths in an aluminium sample and polishing the surface. This ensured that the defects were optically invisible from the top surface, where the measurements were made. A defect where 80 μm of material remained was not visible either optically or ultrasonically. This is to be expected as the Rayleigh waves and the two lowest order Lamb modes have almost identical velocities at this thickness, so the defect appears semi-infinite at the 82 MHz frequency used. Fig. 2*a* shows an acoustic image of a 1 mm diameter hole where the metal thickness gradually tapers from 40 to 35 μm (on the right). At the mean thickness the symmetric and antisymmetric modes differ in velocity by ~16%, and the defect now gives strong contrast against the background. The pattern is again formed by interference between the mode-converted Lamb waves; however, refraction at the interface between the solid material and the defect results in considerable aberration as the

symmetric Lamb mode is refracted away from the normal and the antisymmetric mode is refracted towards the normal. The combination of these effects leads to a fairly complex pattern, which is a function of the semi-angle of the excitation arc, the defect depth and the diameter of the defect. The image formation within the defect has been modelled using a ray-tracing approach, which associated a phase to each ray. The simulated image of the defect with constant metal thickness of 36 μm is shown in Fig. 2b. Since the model assumes a constant thickness of metal, the simulated image shows good agreement with the experimental image; the loss of fringe contrast in regions close to the edge of the defect, marked A, where aberration is severe, is clearly predicted. The periodicity of the pattern provides a powerful means of quantifying the depth of the defect.

Discussion: In this Letter we have shown that the non-contacting surface wave microscope can be used to form quantitative images of sub-surface defects. The mechanism involving interference between mode converted Lamb waves is not appropriate in fluid coupled acoustic microscopy for two principal reasons. First, the effective separation between generation and detection points is much smaller in conventional acoustic microscopy, so the waves do not have sufficient distance to form interference fringes with a period of several Rayleigh wavelengths. Secondly, fluid coupling severely attenuates the Lamb waves as demonstrated when water was placed in the groove of the sample used in Fig. 1a; in this case the interference pattern was not apparent, indicating the removal of at least one of the Lamb modes. The new contrast modes and the ability to support unloaded surface waves indicate than non-contacting surface wave microscopy may have an even richer range of contrast mechanisms than its fluid coupled counterpart.

M.G. Somekh, S.D. Sharples, M. Clark and C.W. See (*School of Electrical and Electronic Engineering, University of Nottingham, University Park, Nottingham, NG7 2RD, United Kingdom*)

References

1 CLARK, M., SHARPLES, S.D., SOMEKH, M.G., and LEITCH, A.S.: 'Non-contacting holographic surface acoustic wave microscope', *Electron. Lett.,* 1999, **35**, (4), pp. 346–347

2 YAMANAKA, K., and ENOMOTO, Y.: 'Fringe pattern around surface crack observed with scanning acoustic microscope', *Electron. Lett.,* 1981, **17**, (18), pp. 638–640

3 CLARK, M., SHARPLES, S.D., and SOMEKH, M.G.: 'Fast laser generated Rayleigh wave scanning microscope'. Proc. Ultrasonics Symp., 1998, pp. 1317–1320

4 VIKTOROV, I.A.: 'Rayleigh and Lamb waves: physical theory and applications' (Plenum Press, New York, 1967)